

Supplemental information

Significance of interferon signaling

based on mRNA-microRNA integration and plasma

protein analyses in critically ill COVID-19 patients

Yuki Togami, Hisatake Matsumoto, Jumpei Yoshimura, Tsunehiro Matsubara, Takeshi Ebihara, Hiroshi Matsuura, Yumi Mitsuyama, Takashi Kojima, Masakazu Ishikawa, Fuminori Sugihara, Haruhiko Hirata, Daisuke Okuzaki, and Hiroshi Ogura

Table S1. Patient characteristics of COVID-19 patients in the IFN proteins profile cohort

| | Non-critical (N=22) | Critical | | |
|---|------------------------|---------------------|---------------------|------------------------|
| | | Overall (N=181) | Survivor (N=154) | Non-survivor (N=27) |
| Age, median, IQR | 70 (61.5-73.3) | 66 (56-74.5) | 63.5 (55.75-73) | 74 (70-80) |
| Sex, male (%) | 19 (86.4) | 125 (69.1) | 109 (70.8) | 16 (59.3) |
| BMI, median, IQR | 24.2 (22.3-29.3) | 25.2 (22.9-27.9) | 25.2 (22.9-27.5) | 25.0 (23.5-29.1) |
| Comorbidities, n (%) | | | | |
| Diabetes | 7 (31.8) | 71 (39.2) | 59 (38.3) | 12 (44.4) |
| Hypertension | 11 (50) | 88 (48.6) | 73 (47.4) | 15 (55.6) |
| Hyperlipidemia | 5 (22.7) | 57 (31.4) | 48 (31.2) | 9 (33.3) |
| Hyperuricemia | 4 (18.2) | 19 (10.5) | 16 (10.4) | 3 (11.1) |
| Chronic heart disease | 5 (22.7) | 17 (9.4) | 13 (8.4) | 4 (14.8) |
| Chronic lung disease | 4 (18.2) | 22 (12.2) | 17 (11.0) | 5 (18.5) |
| Chronic kidney disease | 2 (9.1) | 21 (11.6) | 17 (11.0) | 4 (14.8) |
| Immunocompromised condition | 1 (4.5) | 5 (2.7) | 4 (2.6) | 1 (3.7) |
| Malignant neoplasm | 1 (4.5) | 15 (8.3) | 12 (7.8) | 3 (11.1) |
| Length of hospitalization | 10 (6-20) | 11 (8-17) | 10 (7-16) | 17.5 (11.8-34.5) |
| Acuity score | | | | |
| 1= Death | 5 (22.7) | 26 (14.4) | 0 (0) | 27 (100) |
| 2= Intubated/ventilated, survived | 5 (22.7) | 155 (85.6) | 154 (100) | 0 (0) |
| 3= Hospitalized, O ₂ required, survived | 12 (54.5) | 0 (0) | 0 (0) | 0 (0) |
| 4= Hospitalized, no O ₂ required, survived | 0 (0) | 0 (0) | 0 (0) | 0 (0) |
| 5= Discharged/Not hospitalized, survived | 0 (0) | 0 (0) | 0 (0) | 0 (0) |
| Intubation required, n (%) | 9 (40.9) | 181 (100) | 154 (100) | 27 (100) |
| Extracorporeal membrane oxygenation | 1 (12.5) | 8 (4.5) | 6 (3.9) | 2 (7.7) |
| SOFA score, median, IQR | 2 (2-3) | 5 (3-6) | 5 (3-6) | 6 (5-7) |
| APACHE II score, median, IQR | 7 (4-12.5) | 13 (10-15) | 12 (9-15) | 15 (12-20) |
| Clade, n (%) | | | | |
| 20A | 0 (0) | 1 (0.6) | 1 (0.6) | 0 (0) |
| 20B | 3 (13.6) | 19 (10.5) | 17 (11.0) | 2 (7.4) |
| 20I (Alpha, V1) | 0 (0) | 14 (7.7) | 11 (7.1) | 3 (11.1) |
| unknown | 19 (86.4) | 147 (81.2) | 125 (81.2) | 22 (81.5) |

IQR, interquartile range; BMI, body mass index; SOFA, Sequential Organ Failure Assessment; APACHE, Acute Physiology and Chronic Health Evaluation.

Data are shown as group number (percentage) or median (interquartile range).

Table S2. Significant canonical signaling pathways in COVID-19 mRNA identified in the RNA-seq derivation cohort

| Ingenuity Canonical Pathways | -log (B-H p-value) | z-score |
|--|--------------------|---------|
| Interferon Signaling | 10.1 | 3.962 |
| PD-1, PD-L1 Cancer Immunotherapy Pathway | 8.95 | 2.333 |
| TREM1 Signaling | 6.92 | 3.413 |
| Neuroinflammation Signaling Pathway | 6.91 | 2.018 |
| MSP-ROn Signaling in Macrophages Pathway | 5.61 | 3.452 |
| Role of PKR in Interferon Induction and Antiviral Response | 5.22 | 3.124 |
| Toll-like Receptor Signaling | 5.22 | 3.838 |
| Role of Pattern Recognition Receptors in Recognition of Bacteria and Viruses | 5.19 | 2.746 |
| Role of Hypercytokinemia/Hyperchemokineemia in the Pathogenesis of Influenza | 4.83 | 4.382 |
| Production of Nitric Oxide and Reactive Oxygen Species in Macrophages | 4.42 | 2.48 |
| Osteoarthritis Pathway | 3.46 | 2.402 |
| iNOS Signaling | 3.35 | 3.357 |
| p38 MAPK Signaling | 3.18 | 3.772 |
| Inflammasome Pathway | 2.75 | 3.162 |
| IL-8 Signaling | 2.45 | 2.03 |
| CREB Signaling in Neurons | 2.39 | -2.223 |
| IL-6 Signaling | 2.27 | 2.921 |
| Acute Phase Response Signaling | 2.16 | 3.528 |
| Cyclins and Cell Cycle Regulation | 2.12 | 2.236 |
| Salvage Pathways of Pyrimidine Ribonucleotides | 1.94 | 2.041 |
| Estrogen-mediated S-phase Entry | 1.91 | 2.53 |
| Fcγ Receptor-mediated Phagocytosis in Macrophages and Monocytes | 1.89 | 2.041 |
| GPCR-Mediated Nutrient Sensing in Enteroendocrine Cells | 1.86 | -2.117 |
| Ephrin Receptor Signaling | 1.64 | 2.4 |
| Salvage Pathways of Pyrimidine Deoxyribonucleotides | 1.62 | 2 |
| Nitric Oxide Signaling in the Cardiovascular System | 1.49 | -2.236 |
| Autophagy | 1.31 | 2.343 |

Table S3. Significant canonical signaling pathways in miRNA-targeted mRNA expressions in the RNA-seq derivation cohort

| Ingenuity Canonical Pathways | -log (B-H p-value) | z-score |
|--|--------------------|---------|
| PD-1, PD-L1 Cancer Immunotherapy Pathway | 3.92 | 2.5 |
| MSP-RON Signaling in Macrophages Pathway | 3.84 | 2.837 |
| p38 MAPK Signaling | 3.27 | 2.683 |
| Interferon Signaling | 2.88 | 2.53 |
| Osteoarthritis Pathway | 1.8 | 2.183 |
| Role of Hypercytokinemia/Hyperchemokineemia in the Pathogenesis of Influenza | 1.32 | 2.887 |

Table S4. Significant canonical signaling pathways in COVID-19 mRNA identified in the RNA-seq validation cohort

| Ingenuity Canonical Pathways | -log (B-H p-value) | z-score |
|--|--------------------|---------|
| EIF2 Signaling | 16 | -4.025 |
| Interferon Signaling | 10.3 | 4.264 |
| Neuroinflammation Signaling Pathway | 8.77 | 3.491 |
| PD-1, PD-L1 Cancer Immunotherapy Pathway | 8.2 | 2.197 |
| Pyroptosis Signaling Pathway | 7.61 | 4.226 |
| TREM1 Signaling | 7.6 | 3.413 |
| Role of PKR in Interferon Induction and Antiviral Response | 7.53 | 3.042 |
| STAT3 Pathway | 6.63 | 2.6 |
| Fcγ Receptor-mediated Phagocytosis in Macrophages and Monocytes | 6.52 | 3.307 |
| Autophagy | 6.19 | 3.641 |
| Inflammasome Pathway | 5.87 | 2.496 |
| NAD Signaling Pathway | 5.28 | 2.53 |
| Production of Nitric Oxide and Reactive Oxygen Species in Macrophages | 5.15 | 2.111 |
| Phagosome Formation | 4.86 | 2.025 |
| IL-8 Signaling | 4.64 | 3.395 |
| Role of Hypercytokinemia/Hyperchemokineemia in the Pathogenesis of Influenza | 4.44 | 4.426 |
| MSP-ROn Signaling in Macrophages Pathway | 4.38 | 3.307 |
| Toll-like Receptor Signaling | 4.31 | 3.638 |
| Role of Pattern Recognition Receptors in Recognition of Bacteria and Viruses | 4.31 | 2.858 |
| iNOS Signaling | 4.2 | 3.357 |
| Salvage Pathways of Pyrimidine Deoxyribonucleotides | 3.87 | 2.449 |
| Necroptosis Signaling Pathway | 3.52 | 3.244 |
| Tumor Microenvironment Pathway | 3.26 | 2.03 |
| p38 MAPK Signaling | 3.17 | 2.746 |
| Regulation of Actin-based Motility by Rho | 2.95 | 2.294 |
| Signaling by Rho Family GTPases | 2.85 | 2.082 |
| Ephrin Receptor Signaling | 2.54 | 3.888 |
| GM-CSF Signaling | 2.38 | 2.183 |
| Retinoic Acid Mediated Apoptosis Signaling | 2.35 | 2.183 |
| Endocannabinoid Cancer Inhibition Pathway | 2.35 | 2.694 |
| IL-6 Signaling | 2.31 | 2.887 |
| Kinetochore Metaphase Signaling Pathway | 2.28 | 2.041 |
| Phosphatidylglycerol Biosynthesis II (Non-plastidic) | 2.26 | 2.53 |
| Role of MAPK Signaling in Promoting the Pathogenesis of Influenza | 2.19 | 3.138 |
| Acute Phase Response Signaling | 2 | 3.286 |

| | | |
|---|------|--------|
| Acute Phase Response Signaling | 2 | 3.286 |
| CDP-diacylglycerol Biosynthesis I | 1.97 | 2.333 |
| Colorectal Cancer Metastasis Signaling | 1.95 | 2.214 |
| Actin Cytoskeleton Signaling | 1.94 | 2.333 |
| Epithelial Adherens Junction Signaling | 1.89 | 2.828 |
| Chondroitin and Dermatan Biosynthesis | 1.89 | 2 |
| RHO GDI Signaling | 1.88 | -2.117 |
| Remodeling of Epithelial Adherens Junctions | 1.86 | 2.828 |
| Gai Signaling | 1.84 | 2.294 |
| 3-phosphoinositide Degradation | 1.84 | 2.335 |
| HMGB1 Signaling | 1.8 | 2.2 |
| BEX2 Signaling Pathway | 1.8 | -2.357 |
| IL-1 Signaling | 1.64 | 2.111 |
| Unfolded protein response | 1.64 | 3 |
| D-myo-inositol (1,4,5,6)-tetrakisphosphate Biosynthesis | 1.61 | 2.268 |
| D-myo-inositol (3,4,5,6)-tetrakisphosphate Biosynthesis | 1.61 | 2.268 |
| D-myo-inositol-5-phosphate Metabolism | 1.54 | 2.191 |
| Insulin Secretion Signaling Pathway | 1.51 | 3.063 |
| Ceramide Signaling | 1.39 | 2.183 |
| Oncostatin M Signaling | 1.38 | 3.317 |
| LPS-stimulated MAPK Signaling | 1.34 | 2.668 |
| Triacylglycerol Biosynthesis | 1.31 | 2.714 |
| Wound Healing Signaling Pathway | 1.3 | 3.507 |
| Semaphorin Neuronal Repulsive Signaling Pathway | 1.3 | 2.041 |

Table S5. Significant canonical signaling pathways in miRNA-targeted mRNA expressions in the RNA-seq validation cohort

| Ingenuity Canonical Pathways | -log (B-H p-value) | z-score |
|--|--------------------|---------|
| Autophagy | 7.29 | 2.795 |
| Interferon Signaling | 5.51 | 3.464 |
| Fcγ Receptor-mediated Phagocytosis in Macrophages and Monocytes | 5.48 | 3.273 |
| Phagosome Formation | 4.82 | 2.692 |
| IL-8 Signaling | 4.27 | 3.545 |
| Production of Nitric Oxide and Reactive Oxygen Species in Macrophages | 3.91 | 2.2 |
| iNOS Signaling | 3.6 | 2.333 |
| MSP-ROn Signaling In Macrophages Pathway | 3.15 | 2.524 |
| Integrin Signaling | 2.87 | 2.558 |
| Role of Hypercytokinemia/hyperchemokine in the Pathogenesis of Influenza | 2.86 | 2.84 |
| Pyroptosis Signaling Pathway | 2.54 | 2.84 |
| Protein Kinase A Signaling | 2.44 | -2.263 |
| Hypoxia Signaling in the Cardiovascular System | 2.11 | 2 |
| Salvage Pathways of Pyrimidine Deoxyribonucleotides | 2.08 | 2 |
| Signaling by Rho Family GTPases | 1.96 | 2.828 |
| Regulation of Actin-based Motility by Rho | 1.82 | 2.309 |
| Ephrin Receptor Signaling | 1.79 | 3.9 |
| IL-17A Signaling in Gastric Cells | 1.78 | 2 |
| LPS-stimulated MAPK Signaling | 1.76 | 2.309 |
| Toll-like Receptor Signaling | 1.63 | 2.121 |
| IL-6 Signaling | 1.52 | 2.84 |
| Actin Nucleation by ARP-WASP Complex | 1.52 | 2.828 |
| Insulin Secretion Signaling Pathway | 1.52 | 2.746 |
| Tumor Microenvironment Pathway | 1.51 | 2.065 |
| Ephrin B Signaling | 1.48 | 2.121 |
| Acute Phase Response Signaling | 1.39 | 2.84 |
| 3-phosphoinositide Degradation | 1.32 | 2.324 |
| D-myo-inositol (1,4,5,6)-Tetrakisphosphate Biosynthesis | 1.3 | 2.138 |
| D-myo-inositol (3,4,5,6)-tetrakisphosphate Biosynthesis | 1.3 | 2.138 |

Table S6. Top five statistically significant correlated studies in the BaseSpace Correlation Engine Analysis using mRNA gene expressions in the RNA-seq derivation cohort

| Study name | Public Id |
|--|------------------|
| Study 1: Blood biomarker signature for the diagnosis of septicemic melioidosis | GSE13015 |
| Study 2: Blood transcriptional diagnostic assay for septicemic melioidosis | GSE69528 |
| Study 3: Systemic lupus erythematosus blood samples with different anti-Ro60 titers and interferon metrics | GSE72509 |
| Study 4: Whole blood transcriptional modules for 9 different pathologies | GSE29536 |
| Study 5: Blood gene expression profiles of tuberculosis patients and infected healthy donors | GSE28623 |

For details on each Study, see Table S6-2.

Table S7. Top five statistically significant correlated studies in the BaseSpace Correlation Engine Analysis using miRNA-targeted mRNA gene expressions in the RNA-seq derivation cohort

| Study name | Public Id |
|---|------------------|
| Study 1: Blood biomarker signature for the diagnosis of septicemic melioidosis | GSE13015 |
| Study 2: Blood transcriptional diagnostic assay for septicemic melioidosis | GSE69528 |
| Study 3: Whole blood gene expression in response to dengue disease | GSE28405 |
| Study 4: Whole blood of juvenile idiopathic arthritis and inflammatory bowel disease patients | GSE112057 |
| Study 5: Whole blood transcriptional modules for 9 different pathologies | GSE29536 |

For details on each Study, see Table S7-2.

Table S8. Top five statistically significant correlated studies in the BaseSpace Correlation Engine Analysis using mRNA gene expressions in the RNA-seq validation cohort

| Study name | Public Id |
|--|------------------|
| Study 1: Whole blood of sepsis survivors and nonsurvivors | GSE54514 |
| Study 2: Blood biomarker signature for the diagnosis of septicemic melioidosis | GSE13015 |
| Study 3: Blood transcriptional diagnostic assay for septicemic melioidosis | GSE69528 |
| Study 4: Blood gene expression in sepsis patients compared to healthy subjects and patients post-surgery | GSE28750 |
| Study 5: Whole blood gene expression in response to dengue disease | GSE28405 |

For details on each Study, see Table S8-2.

Table S9. Top five statistically significant correlated studies in the BaseSpace Correlation Engine Analysis using miRNA-targeted mRNA gene expressions in the RNA-seq validation cohort

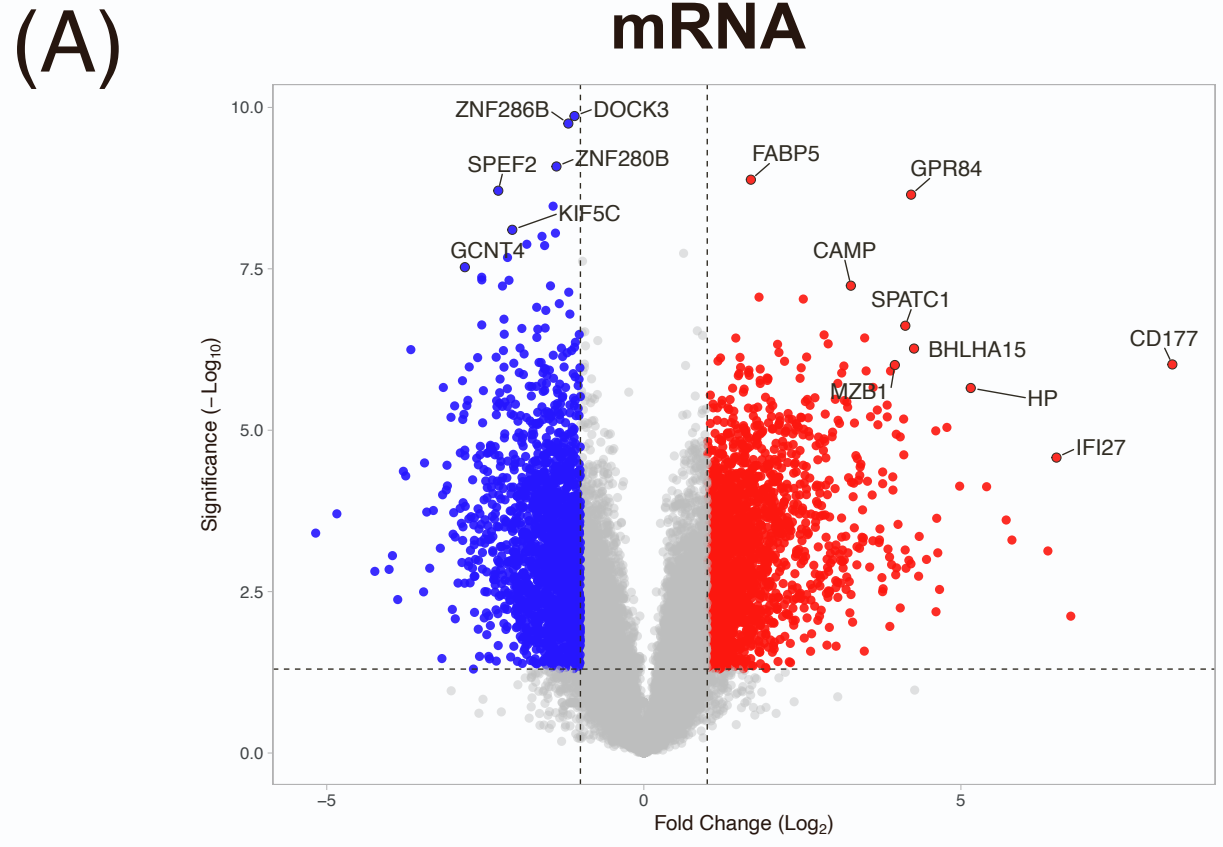
| Study name | Public Id |
|--|------------------|
| Study 1: Blood biomarker signature for the diagnosis of septicemic melioidosis | GSE13015 |
| Study 2: Blood transcriptional diagnostic assay for septicemic melioidosis | GSE69528 |
| Study 3: Whole blood of sepsis survivors and nonsurvivors | GSE54514 |
| Study 4: Whole blood gene expression in response to dengue disease | GSE28405 |
| Study 5: Systemic Lupus Erythematosus trial of Tabalumab | GSE88887 |

For details on each Study, see Table S9-2.

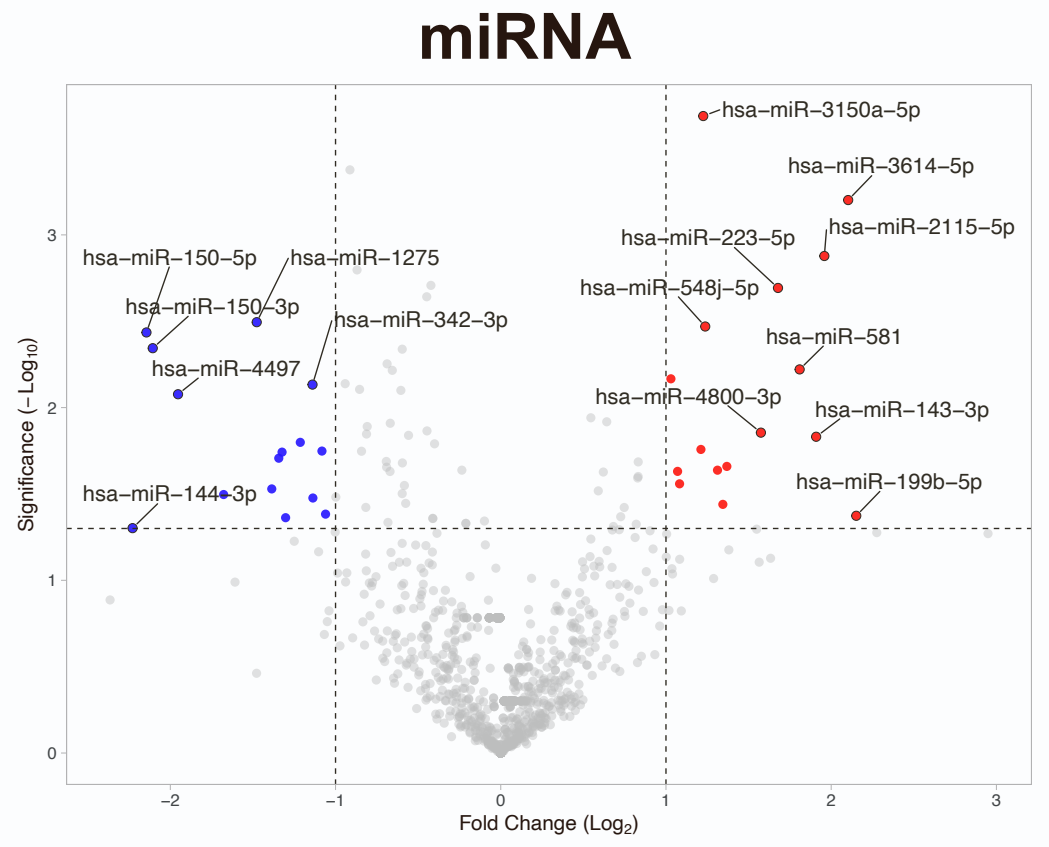
Table S10. List of qPCR primers used for technical validation.

| Primer name | Sequence 5' to 3' |
|----------------------|--------------------------|
| STAT1 forward | TGTATGCCATCCTCGAGAGC |
| STAT1 reverse | AGACATCCTGCCACCTTGTG |
| STAT3 forward | GGCCCCTCGTCATCAAGA |
| STAT3 reverse | TTTGACCAGCAACCTGACTTTAGT |
| IL-1 β forward | CGCAGGACAGGTACAGATTCTT |
| IL-1 β reverse | AAAAAGCTTGGTGATGTCTGGT |
| GADPH forward | CTCTGCTCCTCCTGTTTCGAC |
| GADPH reverse | ACGACCAAATCCGTTGACTC |

Figure S1



Up-regulation 1747
Down-regulation 1741



Up-regulation 16
Down-regulation 15

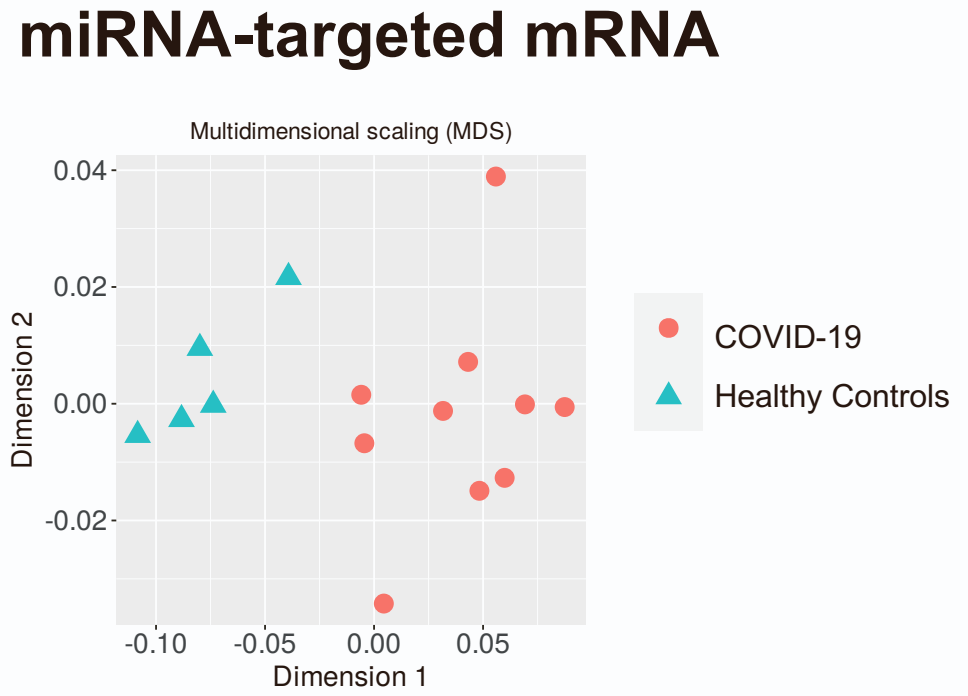
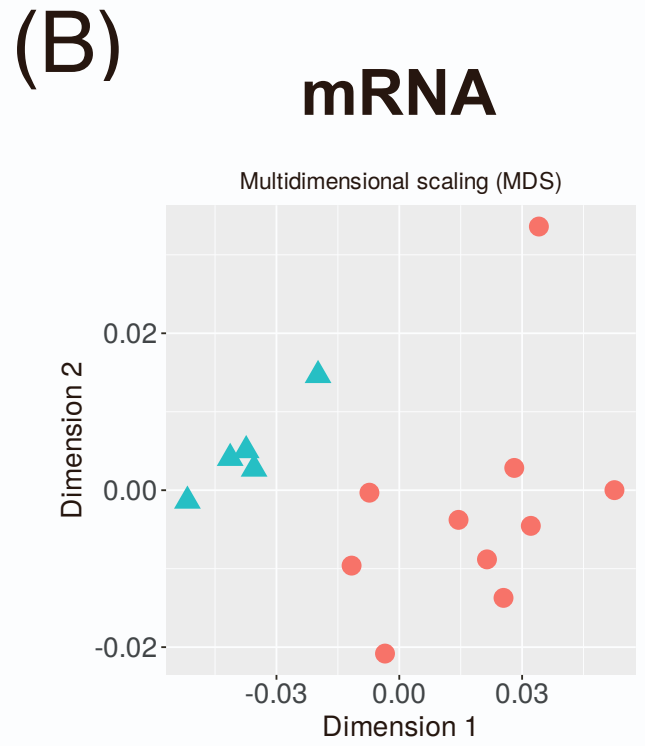
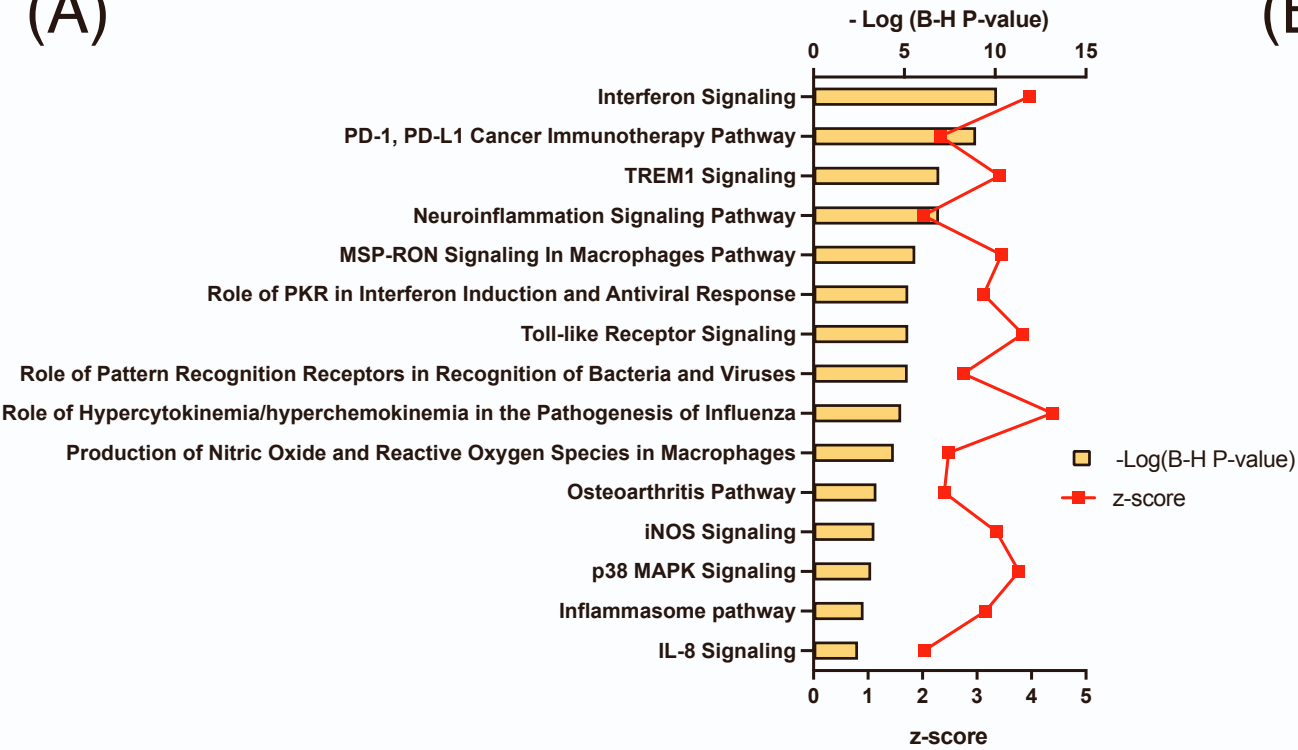


Figure S1. Volcano plot and multidimensional scaling analyses for mRNA, miRNA and miRNA-targeted mRNA expressions in the RNA-seq derivation cohort

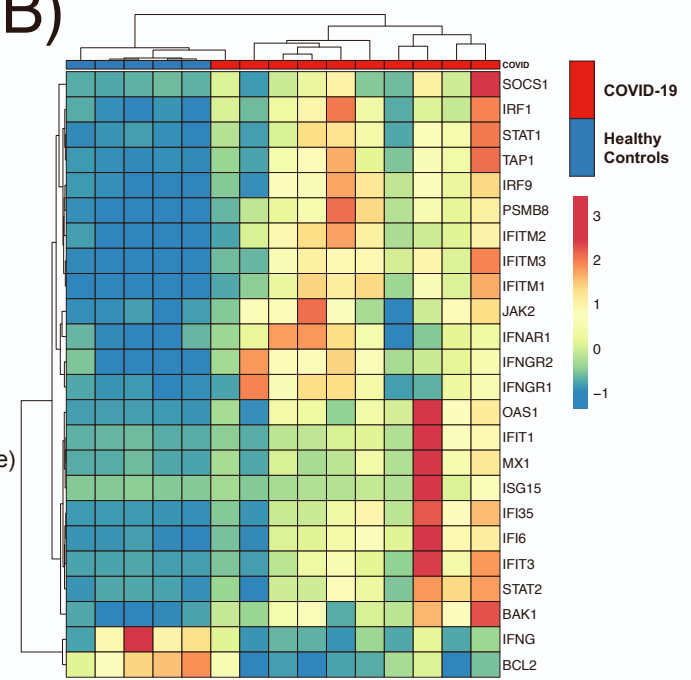
(A) Volcano plot representing the differentially expressed mRNA and miRNA expressions in COVID-19 as compared to the healthy controls. Among the differentially expressed RNA expressions, 1747 mRNA and 16 miRNA expressions were up-regulated and 1741 mRNA and 15 miRNA expressions were down-regulated. The significant differentially expressed RNA expressions are indicated. The vertical dotted lines represent $|\log_2 \text{fold change}| > 1$. The horizontal dotted line represents the threshold for $p < 0.05$. Red dots indicate up-regulated RNA expressions, and blue dots, down-regulated RNA expressions. (B) Multidimensional scaling plot of all mRNA, miRNA and miRNA-targeted mRNA expressions in COVID-19 as compared to the healthy control. COV, COVID-19 patients; HC, healthy controls.

Figure S2

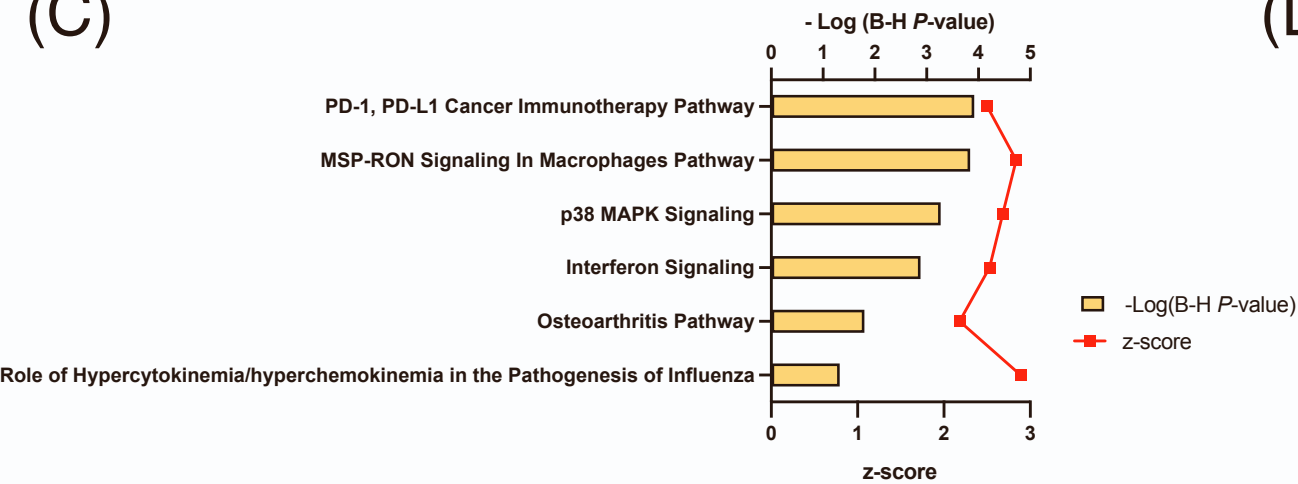
(A)



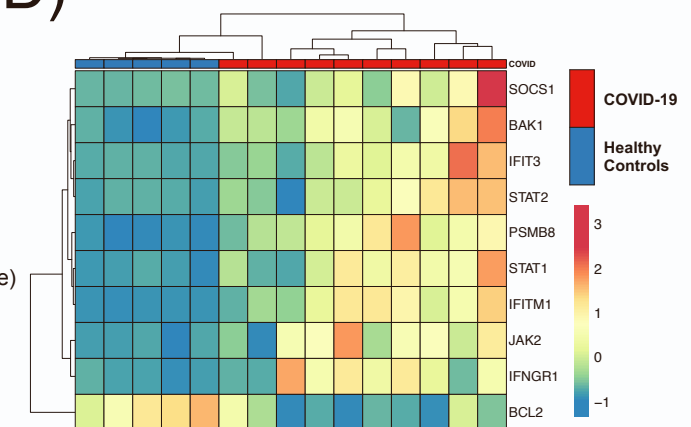
(B)



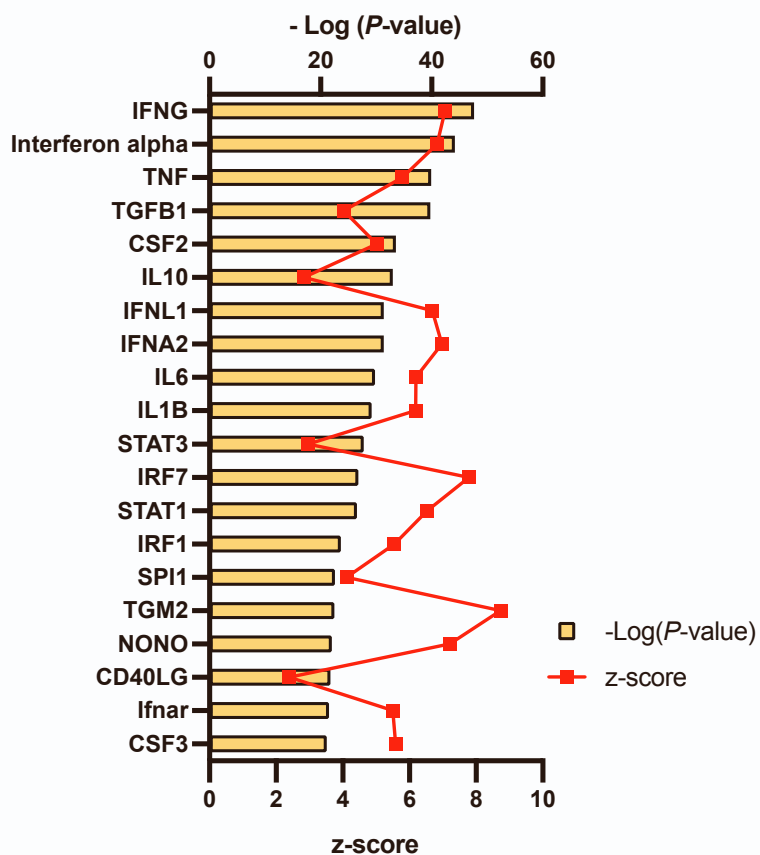
(C)



(D)



(E)



(F)

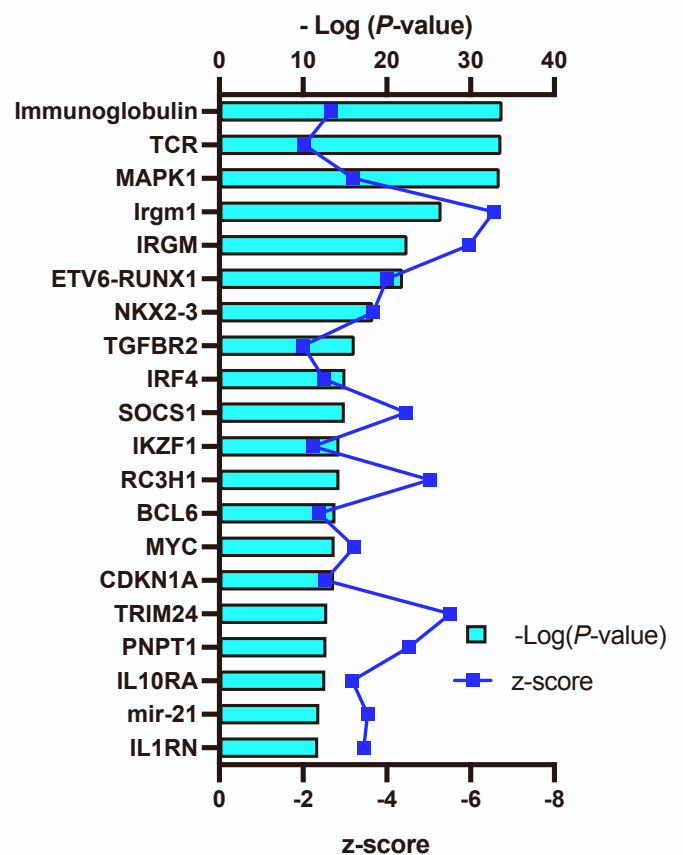
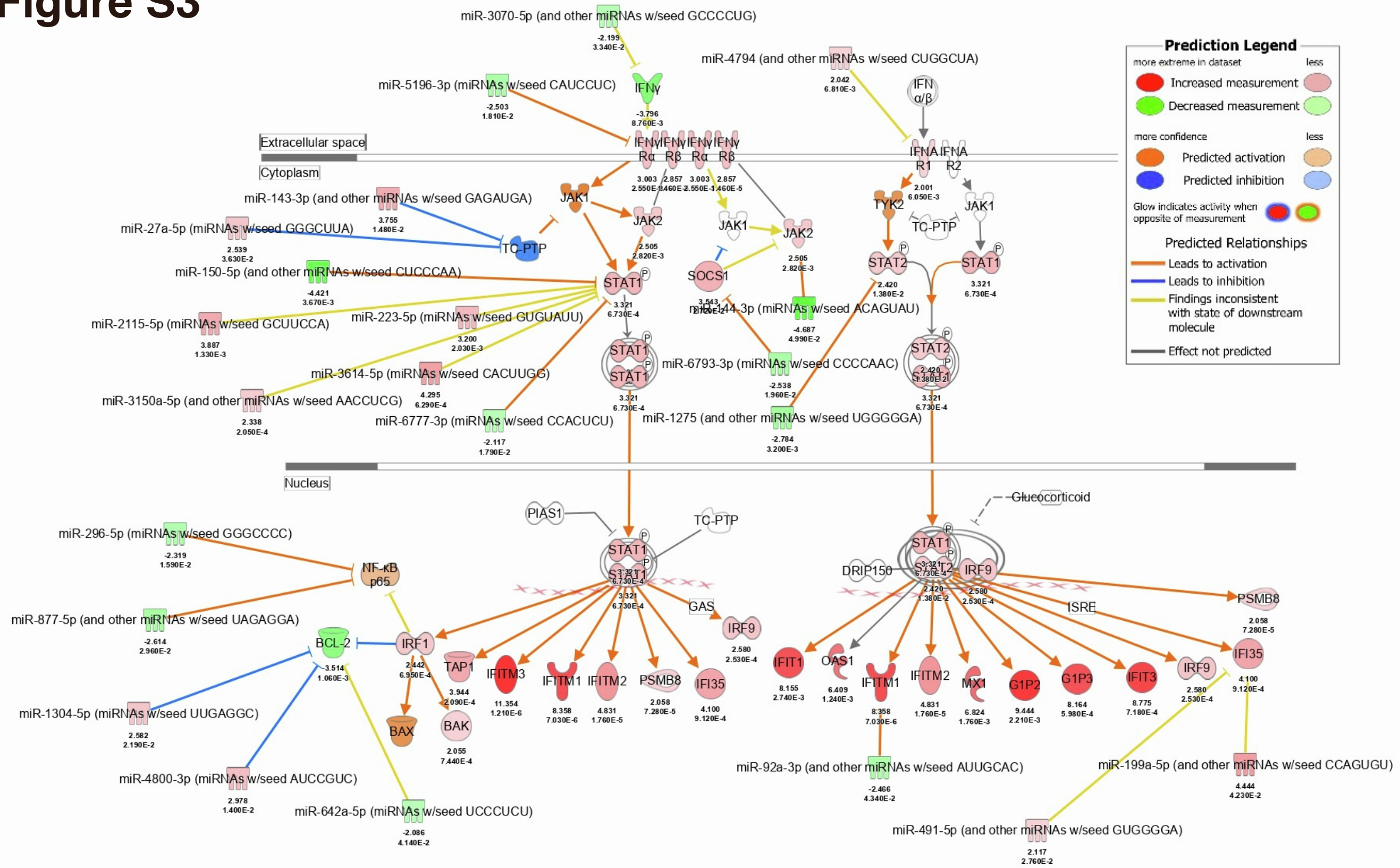


Figure S2. Canonical pathway and upstream analysis in the RNA-seq derivation cohort

(A) Top 15 activated canonical signaling pathways in COVID-19 mRNA identified using Ingenuity Pathway Analysis. (B) Heatmap of gene expression as calculated through RNA-seq involved in the interferon signaling pathway of the samples. (C) Five activated canonical pathways in miRNA-targeted mRNA expressions. (D) Heatmap of gene expression of miRNA-targeted mRNA expressions involved in the interferon signaling pathway of the samples. (E) Top 20 activated upstream regulators. (F) Top 20 inhibited upstream regulators. PD-1, programmed death-1; PD-L1, programmed death-ligand 1; TREM1, triggering receptor expressed on myeloid cells 1; MSP-RON, macrophage-stimulating protein-recepteur d'origine nantais; PKR, protein kinase R; iNOS, inducible nitric oxide synthase; MAPK, mitogen-activated protein kinase; IL, interleukin.

Figure S3

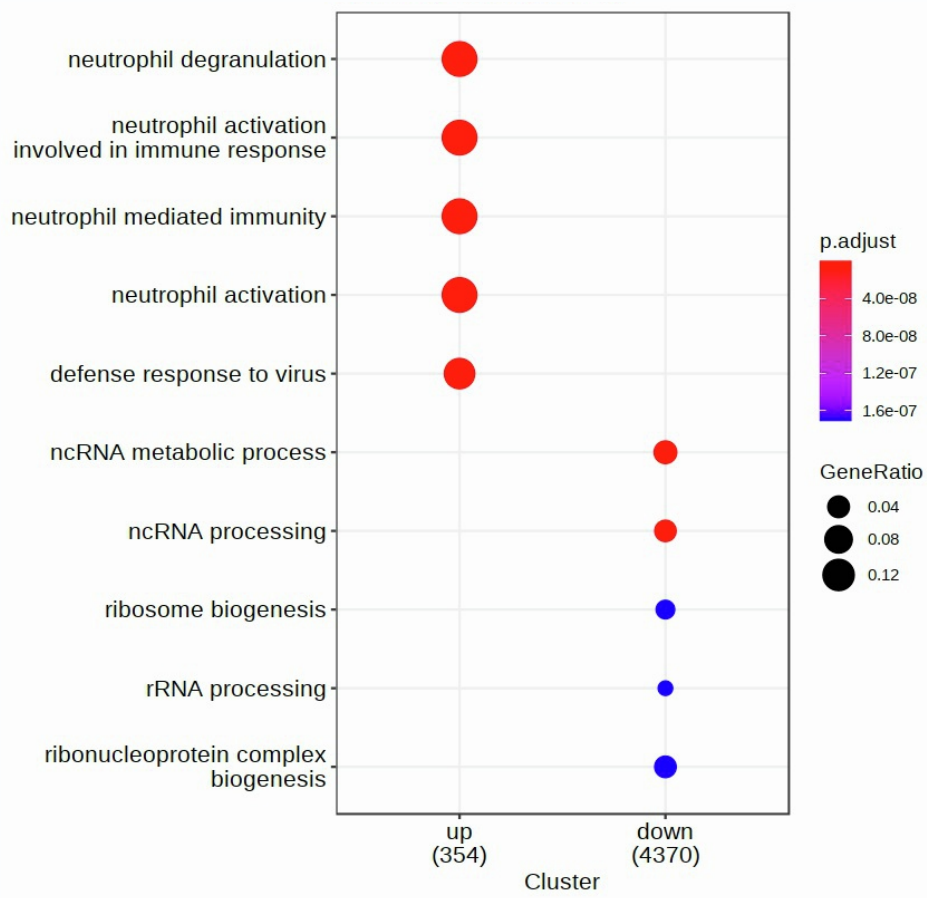


**Figure S3. The activated interferon pathway predicted by Ingenuity Pathway Analysis
in the RNA-seq derivation cohort**

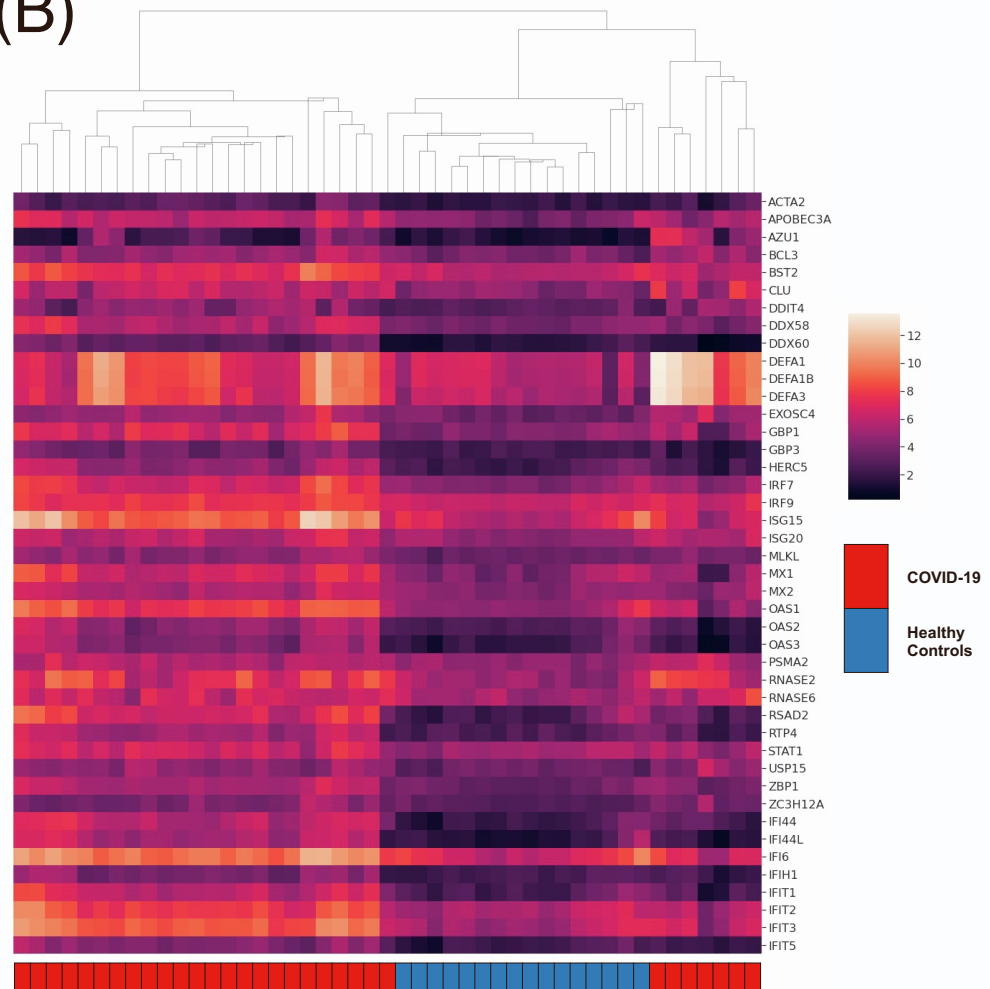
Twenty-five mRNAs and 17 miRNAs with $p < 0.05$, $|\log_2 \text{fold change}| > 1$ were included in the activated interferon pathway.

Figure S4

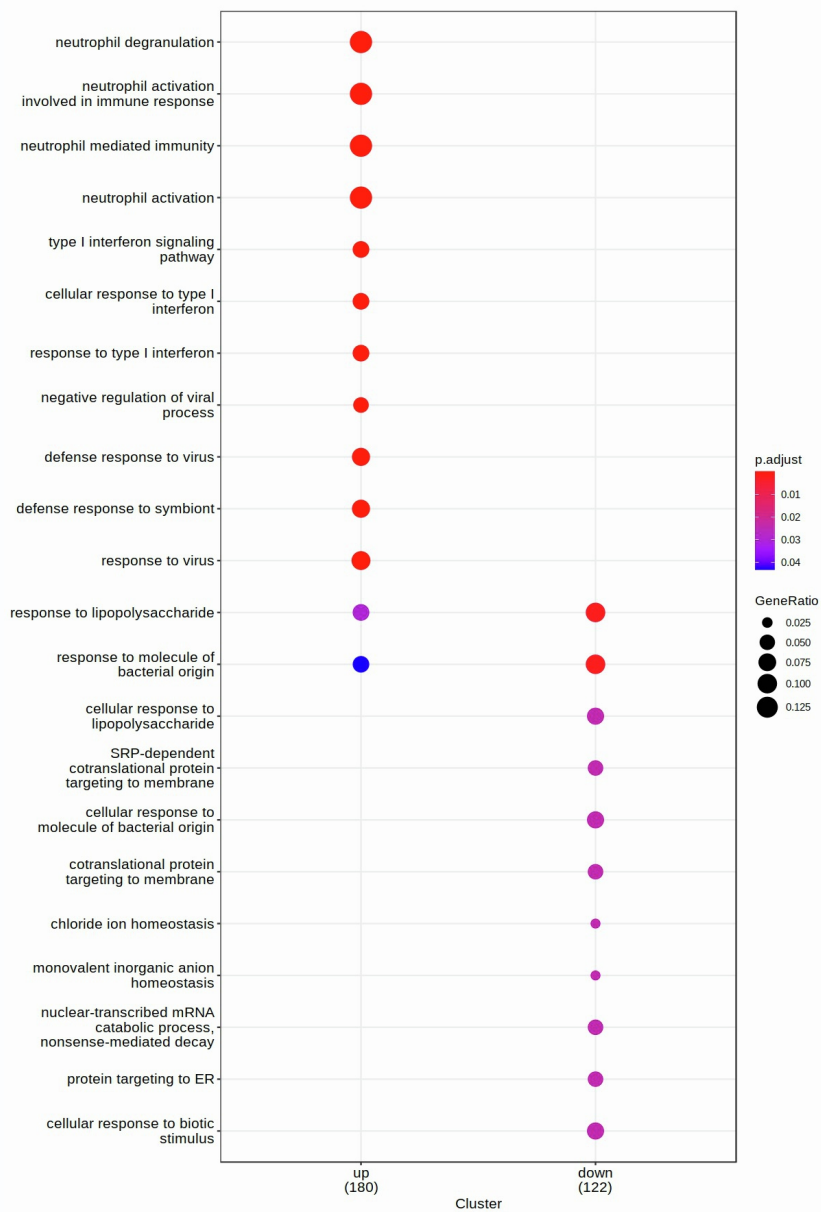
(A)



(B)



(C)



(D)

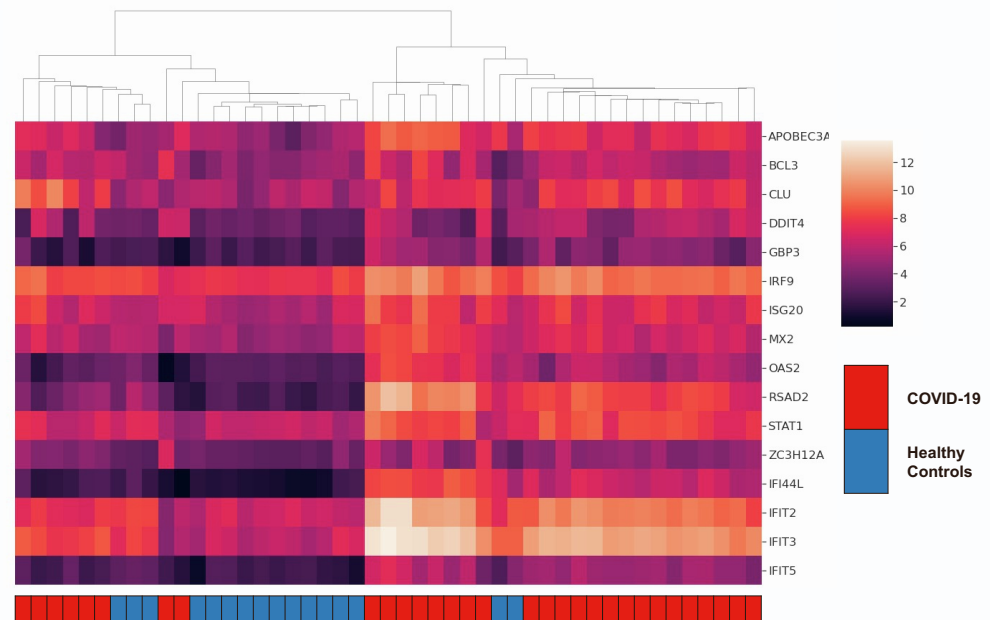
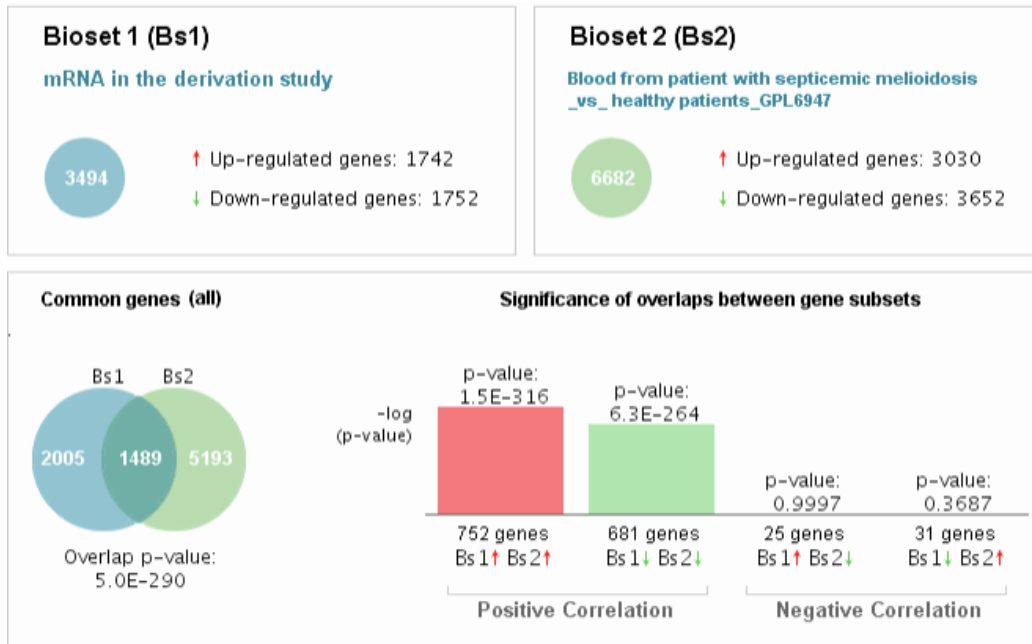


Figure S4. Gene Set Enrichment Analysis (GSEA) in the RNA-seq validation cohort

(A) Dot plot of top five most enriched Gene Ontology (GO) terms for significantly upregulated and downregulated in mRNAs. (B) Heatmap of gene expression of mRNA expressions involved in response to virus. (C) Dot plot of enriched GO terms for significantly upregulated and downregulated in miRNA-targeted mRNAs. (D) Heatmap of gene expression of miRNA-targeted mRNA expressions involved in response to virus.

Figure S5

(A)



(B)

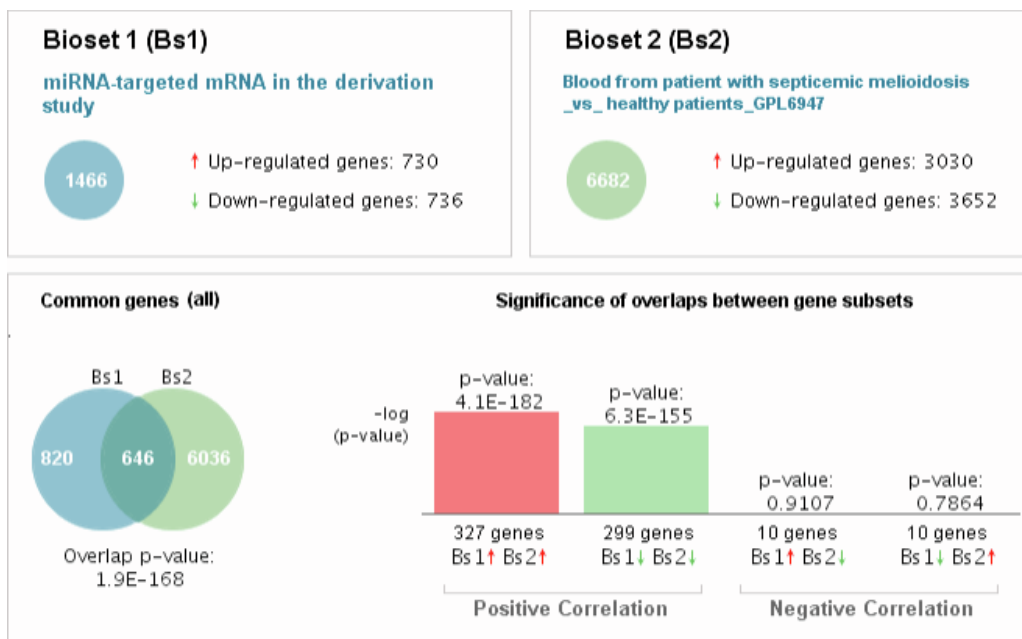
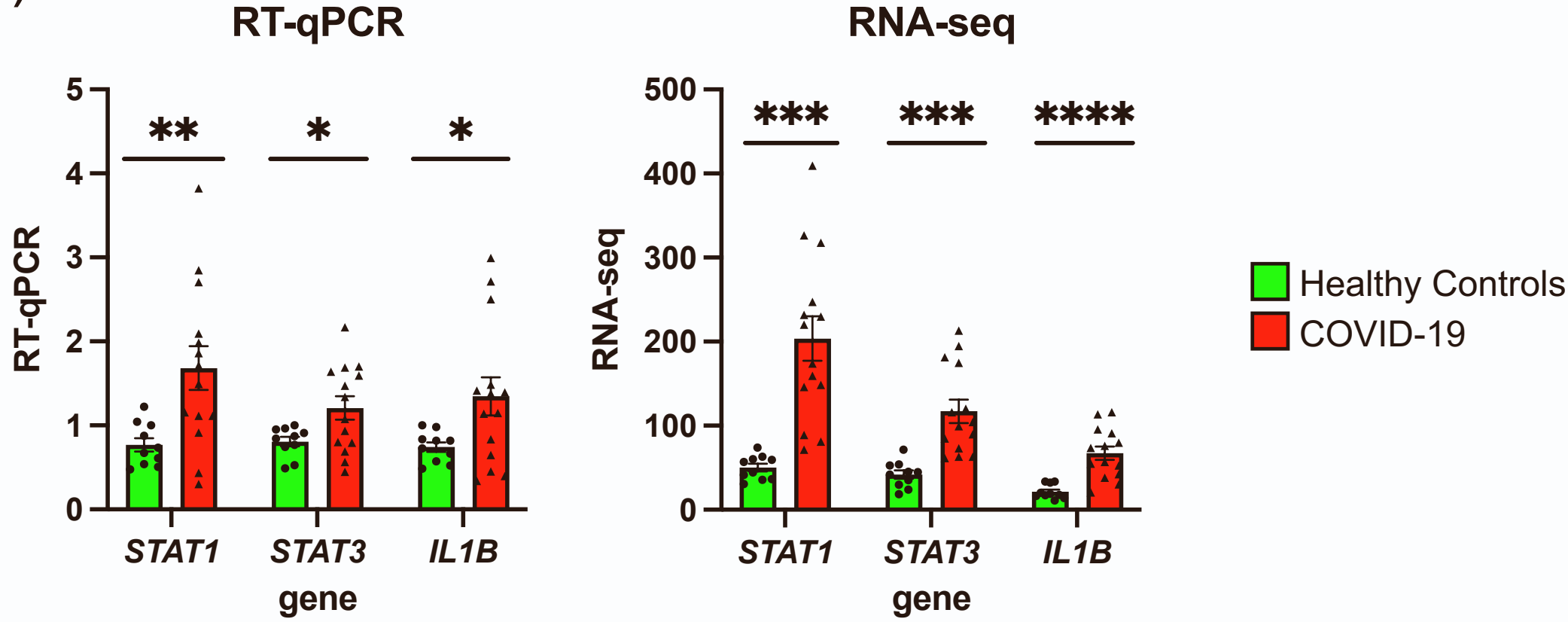


Figure S5. BaseSpace Correlation Engine analysis of the expressions of mRNA and miRNA-targeted mRNA genes in the RNA-seq derivation cohort as compared to the healthy control

The patterns of changes in the expression of genes in the COVID-19 patients in this study [(A) mRNA gene expressions and (B) miRNA-targeted mRNA gene expressions] are compared to the patients with melioidosis. Venn diagrams illustrate the overlap in genome-wide changes in gene expression between the COVID-19 patients and the patients with melioidosis. Bar graphs depict the $-\log$ of the overlap P values for up-regulated (red arrows) or down-regulated (green arrows) genes.

Figure S6

(A)



(B)

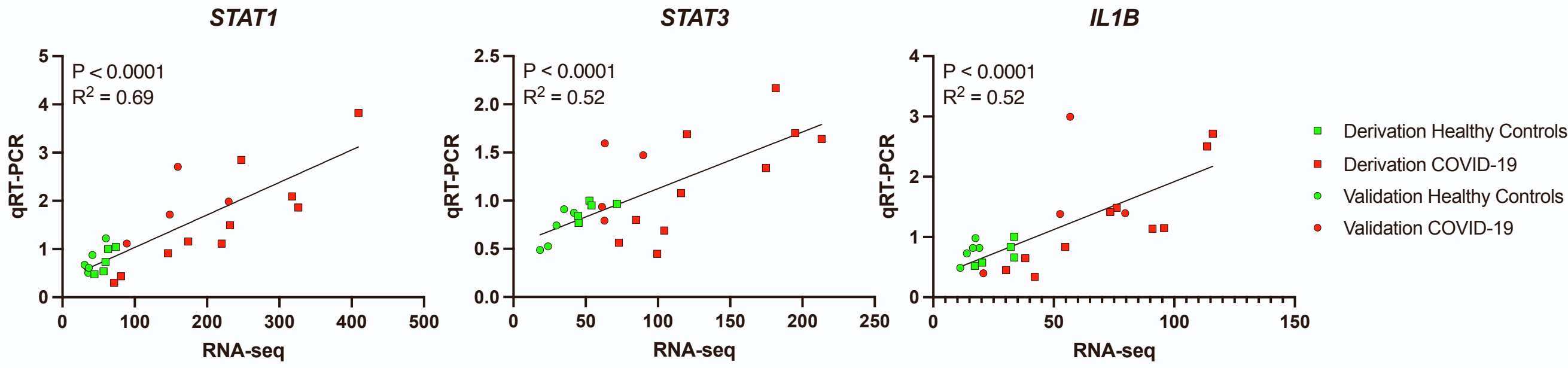


Figure S6. Validation of RNA-Sequencing results by quantitative RT-PCR

(A) Gene expression levels determined by RNA-seq and RT-PCR of three selected upstream regulators (*STAT1*, *STAT3*, *IL1B*) in healthy control subjects and COVID samples. (B)

Correlation between RNA-Seq and RT-PCR gene expression (*STAT1*; $R^2 = 0.69$, $p < 0.0001$.

STAT3; $R^2 = 0.52$, $p < 0.0001$. *IL1B*; $R^2 = 0.52$, $p < 0.0001$).